Anderson localization on Falicov-Kimball model with next-nearest-neighbor hopping and long-range correlated disorder

D. O. Maionchi,[1] A. M. C. Souza,[2] H. J. Herrmann,[1,3] and R. N. da Costa Filho[1]
[1]*Departamento de Física, Universidade Federal do Ceará, 60451-970 Fortaleza, CE, Brazil*
[2]*Departamento de Fisica, Universidade Federal de Sergipe, 49100-000 Sao Cristovao, SE, Brazil*
[3]*Computational Physics, IfB, ETH Hönggerberg, HIF E 12, CH-8093 Zürich, Switzerland*
(Received 19 February 2008; published 20 June 2008)

The phase diagram of correlated disordered electron systems is calculated within dynamical mean-field theory for the Anderson-Falicov-Kimball model with nearest-neighbor and next-nearest-neighbor hoppings. The half-filled band is analyzed in terms of the chemical potential of the system using the geometric and arithmetic averages. We also introduce the on-site energies exhibiting a long-range correlated disorder, which generates a system with similar characteristics as the one created by a random independent variable distribution. A decrease in the correlated disorder reduces the extended phase.

DOI: 10.1103/PhysRevB.77.245126 PACS number(s): 71.10.Fd, 71.27.+a, 71.30.+h

I. INTRODUCTION

Many recent works[1–3] have considered a nonperturbative framework to investigate the Mott metal-insulator transition (MIT) (Ref. 4) in lattice electrons with local interaction and disorder using the dynamical mean-field theory (DMFT).[5] For example, the Anderson transition[6,7] has been explored on the Bethe lattice,[8] considering the Hubbard and Falikov-Kimball models. In these studies, the Mott MIT is characterized by opening a gap in the density of states at the Fermi level. At the Anderson localization, the character of the spectrum at the Fermi level changes from a continuous to a dense discrete one.

The study of disordered systems requires the use of probability distribution functions (PDFs). One is usually interested in typical values of these quantities, which are mathematically given by the most probable value of the PDF. The metal and the insulator phases could be detected by analyzing the local density of states (LDOS). In particular, the arithmetic mean of this random one-particle quantity is noncritical at the Anderson transition and hence cannot help us to detect the localization transition. By contrast, the geometric mean gives a better approximation of the averaged value of the LDOS,[8,9] as it vanishes at a critical strength of the disorder and hence provides an explicit criterion for Anderson localization.[5,10–12] Recently, we adopted the Hölder mean to analyze how the averaged LDOS depends on each Hölder parameter that is used. We showed that the averaged LDOS can vanish in the band center at a critical strength of the disorder for a wide variety of averages.[13]

Most of these studies are restricted to the hopping between nearest neighbors (NNs). Recent works suggest that the inclusion of next-nearest-neighbor (NNN) hopping in the model favors the long-range magnetic ordering.[14] The investigation of these effects is particularly interesting. The breaking of particle-hole symmetry, even at half filling, is a generic property of real materials and creates effects on the paramagnetic phase,[15] besides the frustration of the antiferromagnetic phase.[16] The effect of nonrandom NNN hopping becomes evident already in the noninteracting system through an asymmetric density of states, as already derived for an arbitrary hopping on the Bethe lattice.[17]

On the other hand, the long-range correlated disorder can be generated in a variety of stochastic processes in nature.[18] A tight-binding one-dimensional model of electronic states with the on-site energies exhibiting long-range correlated disorder and nonrandom hopping amplitudes was studied in Ref. 19. The presence of an Anderson-like metal-insulator transition was revealed for a finite range of energy values where the Lyapunov coefficient vanishes. The correlation in the disorder favors the emergence of the extended phase.

In this paper, we investigate two different aspects for the Anderson-Falicov-Kimball model. First, considering nearest-neighbor (NN) and next-nearest-neighbor (NNN) hoppings, we analyzed how the presence of the NNN hoppings influences the phase diagram of the ground state of this model using geometric and arithmetic averages. Besides that, we showed how the chemical potential varies as we look at the half-filled band of different systems; the inclusion of the NNN hopping dislocates the half-filled band from the band center, independent of the disorder that is considered. The ground-state phase diagram is also presented for different values of NNN hoppings. In our study the long-range ordered phases are not considered.

Second, we studied the main effects of the long-range correlated disorder (characterized by the exponent α) in the Anderson-Falicov-Kimball model. Unlike the one-dimensional Anderson model, this disorder does not have a great influence on the behavior of the system. We present the ground-state phase diagram for electrons in a half-filled band for different values of this disorder and the dependence of the disorder in terms of the exponent α for a system without Coulomb repulsion. In the pure half-filled Falicov-Kimball model, the Fermi energy for electrons is inside of the correlation (Mott) gap opened by increasing the interaction.[9] We want to examine how the disorder influences this gap.

The pure Falicov-Kimball model describes two species of particles, mobile and immobile, which interact with each other when both are on the same lattice site. This model is the simplest model to study metal-insulator transitions in mixed-valence compounds of rare-earth and transition-metal oxides, ordering in mixed-valence systems, order-disorder

transitions in binary alloys, itinerant magnetism,[20] crystallization, electronic ferroelectricity in mixed-valence compounds, and phase diagrams of metal ammonia solutions.[21] It also captures some aspects of the Mott-Hubbard MIT.[13]

The Anderson-Falicov-Kimball model considers mobile particles that are disturbed by a local random potential, giving rise to a competition between interaction and disorder. The Hamiltonian is written as

$$H = -\sum_{ij} t_{ij} c_i^+ c_j + \sum_i \epsilon_i c_i^+ c_i + U \sum_i f_i^+ f_i c_i^+ c_i, \tag{1}$$

where c_i^+ (c_i) and f_i^+ (f_i) are, respectively, the creation (annihilation) operators for the mobile and immobile fermions (electrons and ions, respectively) at a lattice site i, t_{ij} is the electron transfer integral connecting sites i and j, and U is the Coulomb repulsion that operates when one ion and one electron occupy the same site. We assume

$$t_{ij} = \begin{cases} t_1 & \text{for nearest-neighbor sites} \\ t_2 & \text{for next-nearest-neighbor sites} \\ 0 & \text{otherwise.} \end{cases}$$

The average number of electrons and ions on site i are denoted, respectively, as $n_e = c_i^+ c_i$ and $n_f = f_i^+ f_i$. We consider that the occupation n_f on the ith site has probability p ($0 < p < 1$). It was assumed, for simplicity, that just mobile particles are subjected to the structural disorder.[9] The energy ϵ_i is a random, independent variable, describing the local disorder disturbing the motion of electrons. The model is solved within the DMFT framework.

In Sec. II we present the DMFT approach applied to the Anderson-Falikov-Kimball model.[9] In Sec. III we present the numerical results concerning the ground-state phase diagram for the next-nearest-neighbor hopping case. In Sec VI we discuss the above model for the long-range correlated disorder. Finally in Sec V we present our conclusions.

II. DYNAMICAL MEAN-FIELD THEORY

The formalism is based on the introduction of the hybridization function $\eta(\omega)$, which is a dynamical mean field describing the coupling of a selected lattice site with the rest of the system.[12] The DMFT is calculated from the Hilbert transforms

$$G(\omega) = \int \frac{d\epsilon N_0(\epsilon)}{\eta(\omega) - \epsilon + 1/G(\omega)}, \tag{2}$$

and

$$G(\omega) = \int d\omega' \frac{\rho_q(\omega')}{\omega - \omega'}. \tag{3}$$

where $N_0(\epsilon)$ is the noninteracting density of states and $G(\omega)$ the translationally invariant Green's function.

The ϵ_i-dependent LDOS is written as

$$\rho(\omega, \epsilon_i) = -\frac{1}{\pi} \mathrm{Im}\, G(\omega, \epsilon_i), \tag{4}$$

where $G(\omega, \epsilon_i)$ is the local ϵ_i-dependent Green's function.[9] ϵ_i is considered as an independent random variable characterized by a probability function $P(\epsilon_i) = \Phi(\Delta/2 - |\epsilon_i|)/\Delta$, with Φ as the step function. The parameter Δ is a measure for the disorder strength. From the ϵ_i-dependent LDOS, we introduce the q-Hölder averaged LDOS,

$$\rho_q(\omega) = \left\{ \sum_i [\rho(\omega, \epsilon_i)]^q \right\}^{1/q}, \tag{5}$$

where the subscript q defines the generalized mean. Special cases are, for example, the minimum ($q \to -\infty$), the geometric mean ($q \to 0$), the arithmetic mean ($q = 1$), and the maximum ($q \to \infty$). Equation (5) inserted in Eq. (3) closes the self-consistent DMFT.

A chemical potential μ is introduced only for the mobile subsystem to fix the system in the half-filled band ($n_e = p = 1/2$). For the Bethe lattice in the limit of infinite connectivity K, one can use the scaling $t_1 = t_1^*/\sqrt{K}$ and $t_2 = t_2^*/K$. In the nearest-neighbor hopping case ($t_2 = 0$), the density of states is the semielliptic function $N_0(\epsilon) = \sqrt{4 - (\epsilon/t_1^*)^2}/(2\pi t_1^*)$,[17] where the bandwidth is $4t_1^*$. We can find $\eta(\omega) = t_1^{*2} G(\omega)$.[9] In this case, the ground-state properties in the half-filled band case are solely determined by the quantum states in the band center ($\omega = 0$), and we can determine the transition points in the phase diagram by linearizing the DMFT equations. However, for $t_2 \neq 0$ the symmetry in the band center is absent, and we cannot use a recursive relation within the linearized DMFT.

For the next-nearest-neighbor hopping case ($t_2 \neq 0$), the analytical expression for the density of states on the Bethe lattice is given by[17]

$$N_0(\epsilon) = \Theta(t_1^{*2} + 4t_2^{*2} + 4t_2^* \epsilon) \frac{\sqrt{4 - \lambda_+^2} + \sqrt{4 - \lambda_-^2}}{2\pi \sqrt{t_1^{*2} + 4t_2^{*2} + 4t_2^* \epsilon}}, \tag{6}$$

where $\Theta(\epsilon)$ is the step function and $\lambda_\pm(\epsilon)$ is solution of the equation

$$t_2^* \lambda^2 + t_1^* \lambda - (t_2^* + \epsilon) = 0. \tag{7}$$

III. NEXT-NEAREST-NEIGHBOR HOPPING

We considered that the initial value of $\rho(\omega, \epsilon_i)$ is a uniform distribution with bandwidth $W = 8t_1^*$, then we determined $G(\omega)$ in order to obtain $\eta(\omega)$ and finally the new values of $\rho(\omega, \epsilon_i)$. This loop is performed until we find the stable configuration for $\rho_q(\omega)$. The relation between $G(\omega)$ and $\eta(\omega)$ is obtained in a straightforward way from Eqs. (2) and (6) leading to the result

$$\eta(\omega) = G(\omega) \left\{ \frac{t_2^{*2}}{1 - G(\omega) t_2^*} + \frac{t_1^{*2}[1 - G(\omega) t_2^*]}{[1 - 2G(\omega) t_2^*]^2} \right\}. \tag{8}$$

If we consider fixed values of U and t_2^*/t_1^*, we can observe the dependence of the averaged LDOS on the value of Δ that is used. Some of these results are presented in Fig. 1. We consider the next-nearest-neighbor hopping model ($t_2^*/t_1^* = 0.0$, 0.4, and 1.0). We can see that the behavior of the LDOS is not the same in all cases. In contrast to the case $t_2^*/t_1^* = 0$, if $t_2^*/t_1^* \neq 0$ the $\rho_q(\omega)$ is asymmetric.

A signature of the Anderson localization is the vanishing of $\rho_q(\omega)$ as we increase Δ. The detection of the Anderson

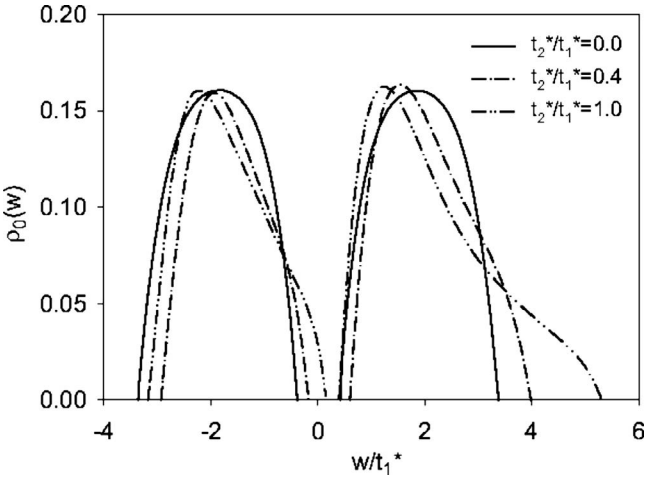

FIG. 1. Averaged local density of states at $U=3.6$ and $q=0$ for (a) $t_2^*/t_1^*=0, 0.4$ and 1.0 for disorder strength $\Delta=2.0$.

localization depends on the average that is used to calculate $\rho_q(\omega)$; using the geometrical average ($q=0$), $\rho_q(\omega)$ vanishes for a certain value of Δ, while using the arithmetical average ($q=1$), the localization cannot be detected. Figure 2 presents the phase diagram of the ground state for the Anderson-Falikov-Kimball model for $U=3.6$ at $t_2=0$ (solid line), $t_2=0.4$ (dash-dotted line), and $t_2=1$ (dash-dot-dotted line) using the geometrical average (black lines) and the arithmetic average (brown lines). It is obtained observing the behavior of the average local density of states for different values of w as the disorder strength Δ is increased. We can identify three regions with respect to the states at the Fermi level: extended gapless phase (continuous spectrum), localized gapless phase (pure point spectrum), and gap phase.[9] The lines delimiting these phases are centered around $w=0$ for $t_2^*/t_1^*=0$, which does not happen for $t_2^*/t_1^*\neq 0$. The asymmetry in the phase

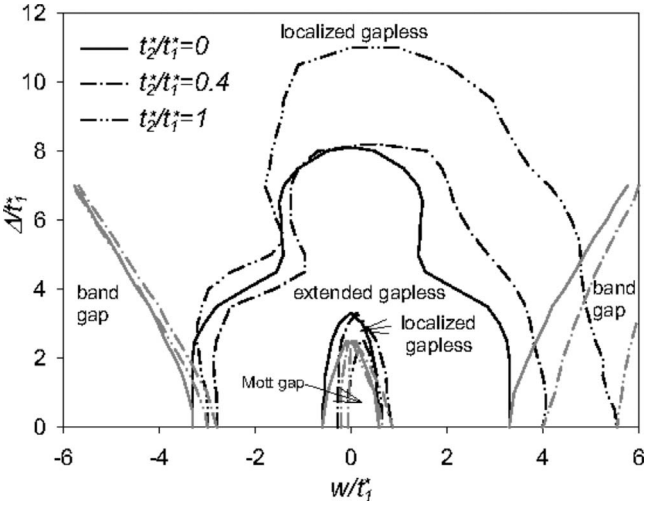

FIG. 2. Phase diagram of the ground state for the Anderson-Falikov-Kimball model for $U=3.6$ at $t_2=0$ (solid line), $t_2^*/t_1^*=0.4$ (dash-dotted line), and $t_2^*/t_1^*=1$ (dash-dot-dotted line). The black lines present mobility edges determined within DMFT with geometric averaging ($q=0$) and the brown lines show band edges determined within DMFT with arithmetic averaging ($q=1$).

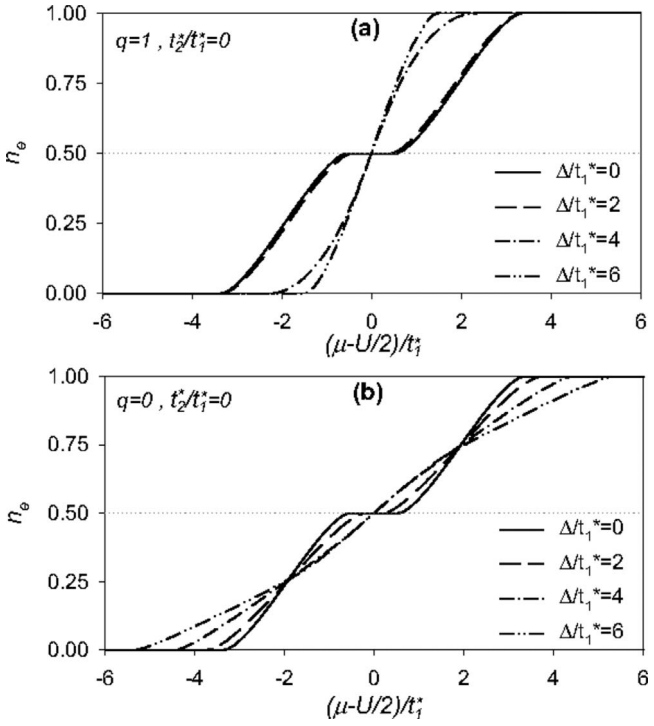

FIG. 3. Averaged electron number n_e versus chemical potential at $U=3.6$ for $t_2^*/t_1^*=0$ and $\Delta=0$, 2.0, 4.0, and 6.0. (a) $q=1$ and (b) $q=0$.

diagram becomes more evident, the higher the value of t_2^*/t_1^*.

As already pointed out, if $t_2\neq 0$, the chemical potential $\mu=U/2$ that was introduced does not affect the system in the half-filled band. When we look at the curves of Fig. 3 obtained for the relation between the chemical potential μ and the average number of electrons n, we see that all the curves obtained for $t_2^*/t_1^*=0$ are centered at $\mu=U/2$ and $n_e=0.5$, independent of the average that is considered. This means that the half-filled band of the system is always in a band center ($\omega=0$) as we vary the disorder Δ of the system. In Fig. 4 we present the curves corresponding to $t_2\neq 0$ ($t_2=0.4$ and $t_2=1.0$) using the geometrical average. We can observe in all curves that for a half-filled band system ($n_e=0.5$), the value of μ does not correspond to $U/2$ anymore, independent of the average that is used and the disorder that is imposed. Since the normalization is lost when we use geometrical averages, we find the chemical potential through $n_e=\int_{-\infty}^{\mu}\rho_0(w)dw/\int_{-\infty}^{\infty}\rho_0(w)dw$.

Figure 5 shows the chemical potential versus disorder parameter Δ for the half-filled band ($n_e=0.5$). We observe that for $t_2^*/t_1^*=0$, the half-filled band is in a band center ($\omega=0$) independent of disorder Δ. As we include the influence of next-nearest-neighbors $t_2^*/t_1^*\neq 0$, the half-filled band is dislocated to bands with $\omega>0$ that correspond to values of μ always greater than $U/2$.

The ground-state phase diagram for electrons in a half-filled band as a function of t_2^*/t_1^* for $U=3.6$ is shown in Fig. 6. Performing the same process for other values of U, we can easily obtain all the simulation points of Fig. 7. In this figure we present a complete ground-state phase diagram for electrons in a half-filled band for three different values of for

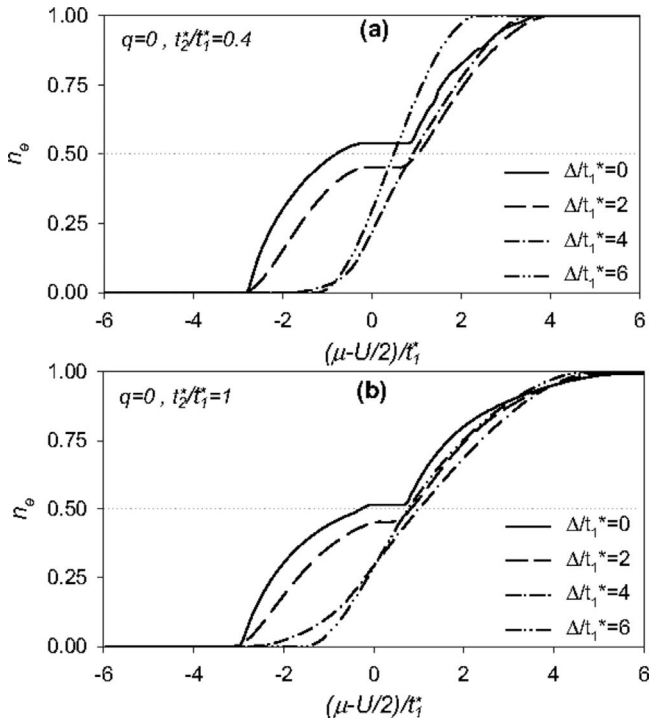

FIG. 4. Averaged electron number n_e versus chemical potential at $U=3.6$ using $q=0$, for $t_2^*/t_1^* \neq 0$ and $\Delta=0$, 2.0, 4.0, and 6.0. (a) $t_2^*/t_1^*=0.4$ and (b) $t_2^*/t_1^*=1.0$.

t_2^*/t_1^*, namely, $t_2^*/t_1^*=0$, 0.4, and 1.0. The presence of t_2 increases the extended phase. The dashed line represents the values of Δ and U where the energy gap goes through the half-filled band. Note that for t_2 different from zero and U large, the extended phase does not disappear because the chemical potential does not correspond to the energy of the gap between the bands. In the limit of large U the density In the limit of large U the density of states is split into two bands. For nonzero t_2 the bands are asymmetric. When we

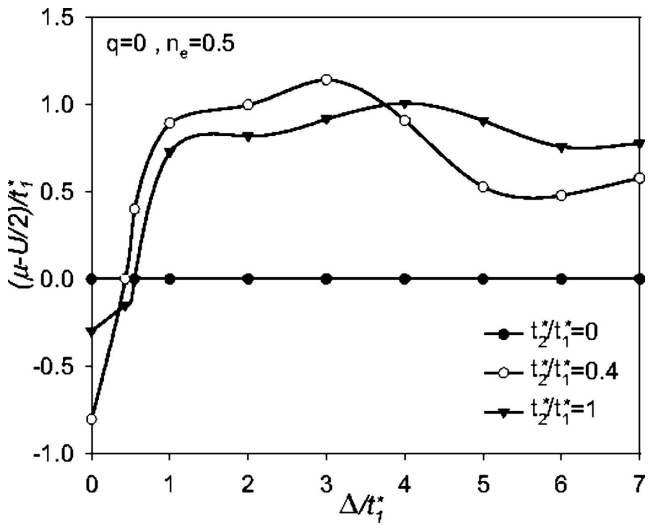

FIG. 5. Chemical potential versus disorder parameter Δ for the half-filled band ($n_e=0.5$). The results are obtained for $t_2^*/t_1^*=0$, 0.4, and 1.0.

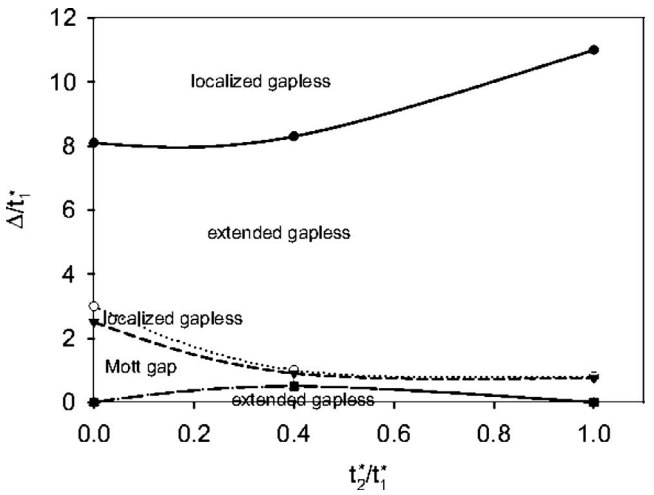

FIG. 6. Ground-state phase diagram for electrons in a half-filled band as a function of t_2^*/t_1^* for $U=3.6$. The dots are determined from the numerical solution of the DMFT equations. The lines are guide to the eye.

set that the immobile particles have $p=1/2$, the DMFT equation of self-consistency for the mobile particles is invariant under a change of the energy axis $w \rightarrow w+\mu-U/2$. Thus, if t_2 is different from zero in the half-filled case ($n_3=1/2$), the chemical potential corresponds to the energy within one of the bands and not to the gap between the bands. Therefore, in this case, the NNN hopping drives the system out of localization at large U. This is a particular property of the Falikov-Kimball model, unlike for example the Hubbard model, where the two fermions that move and the DMFT equation of self-consistency for n_e depend on the equation of consistency for n_f.

IV. LONG-RANGE CORRELATED DISORDER

Recently results[19] have shown that localization properties are modified if correlations are introduced in the disorder

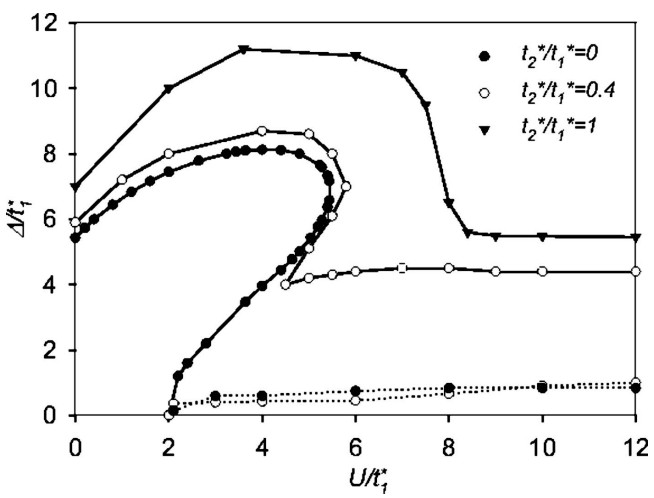

FIG. 7. Ground-state phase diagram for electrons in a half-filled band as a function of U for $t_2^*/t_1^*=0$, 0.4, and 1.0. The dots are determined from the numerical solution of the DMFT equations. The lines are guide to the eye.

distribution. For example, long-range correlated disorder favors the delocalization, giving in one-dimensional systems a range of energies with extended eigenstates. The one-dimensional Anderson model with long-range correlated diagonal disorder displays a phase of extended electronic states where the on-site energy disorder distribution is described by a power-law spectral density.

In what follows, we will study the effect due to long-range correlated disorder in the Anderson-Falicov-Kimball model on the Bethe lattice using the DMFT approach. The energy ϵ_i will not be considered as a random independent variable. Following an approach based on discrete Fourier transforms to construct long-range correlated sequences, the on-site energies can be generated by the expression[19]

$$\epsilon_i = \sum_{k=1}^{N/2} k^{-\alpha/2} \left\| \frac{2\pi}{N} \right\|^{(1-\alpha)/2} \cos\left\{ \frac{2\pi i k}{N} + \phi_k \right\}, \tag{9}$$

where N is the number of sites and ϕ_k are $N/2$ independent random phases uniformly distributed in the interval $[0, 2\pi]$. The uncorrelated disorder is recovered for $\alpha=0$.

The correlation is introduced *a priori* and the correlation is introduced *a priori* and the on-site energies continue to be random variables. The translationally invariant Green's function of the DMFT method can then be used because all sites of the lattice are also equivalent in the correlated disorder that is considered. Other methods that can be used to discuss the phase transitions are the direct diagonalization and the calculation of the participation radius because they use the wave function of the system. For large lattices they can just be applied to $U=0$ and for systems without correlation, we found that the results coincide with those published in the literature.

We will normalize the energy sequence to have the mean value $\langle \epsilon_i \rangle = 0$. The standard deviation is defined as $\sigma = \sqrt{\langle \epsilon_i^2 \rangle - \langle \epsilon_i \rangle^2} = 6\Delta/\sqrt{3}$. For $\alpha=0$, we obtain a Gaussian distribution for the ϵ_i. In this sense, the values of the Coulomb repulsion U and the disorder Δ that we obtain when $\rho_0(w) = 0$ are not the same as obtained with the uniform distribution.

In the case $U=0$, we find in the literature that for the cubic network the transition from the extended states to the localized ones occurs for $\Delta_c=5.5$ for the uniform distribution and $\Delta_c=7.0$ for the Gaussian distribution.[22,23] For the same value of U, we found in our simulations $\Delta_c=5.7$ and 6.8, respectively, for the uniform and the Gaussian distributions. In Fig. 1, we present the ground-state phase diagram for electrons in a half-filled band by using long-range correlated disorder and the geometric average. We see that for different values of α, the diagram that is obtained is similar to the one that corresponds to uncorrelated disorder (Fig. 8).

The difference between the diagrams can be quantified for different values of the exponent α when we look at the value of Δ when $U=0$. The result is presented in Fig. 9. We see that the value of Δ diminishes as the value of α is increased and tends to a constant value for $\alpha>4$. The decrease in Δ means that the correlation reduces the extended phase, different to what happens in low dimension.[19]

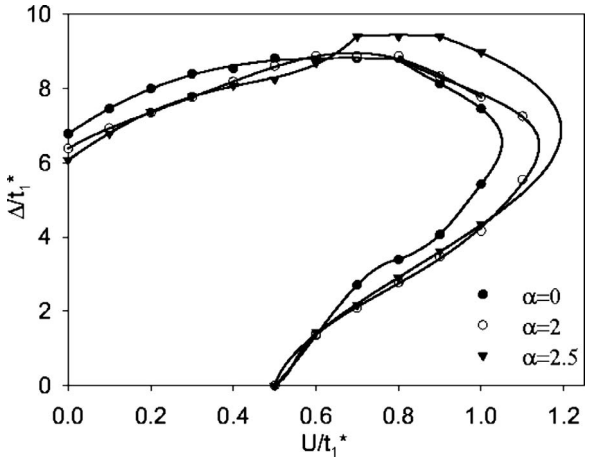

FIG. 8. Ground-state phase diagram for electrons in a half-filled band by using long-range correlated disorder for $\alpha=0$, 2.0, and 2.5. The dots are determined from the numerical solution of the DMFT equations. The lines are guides to the eye.

V. CONCLUSIONS

In the present paper, we studied the solutions of the Anderson-Falicov-Kimball model with NN and NNN hoppings. We found the averaged LDOS calculated using the arithmetic and geometric mean within dynamical mean-field theory. We showed that the inclusion of the NNN with $t_2^*/t_1^* \neq 0$ moves the half-filled band from the band center ($\omega=0$) to bands with $\omega>0$, independent of the disorder Δ that is considered. Besides that the chemical potential μ changes from $U/2$ for $t_2^*/t_1^*=0$ to greater values for $t_2^*/t_1^* \neq 0$.

We also analyzed the behavior of the system when long-range correlated disorder is considered using both the geometric and arithmetic means. We showed that the inclusion of this kind of disorder does not present results different from the ones already obtained for an uncorrelated disorder

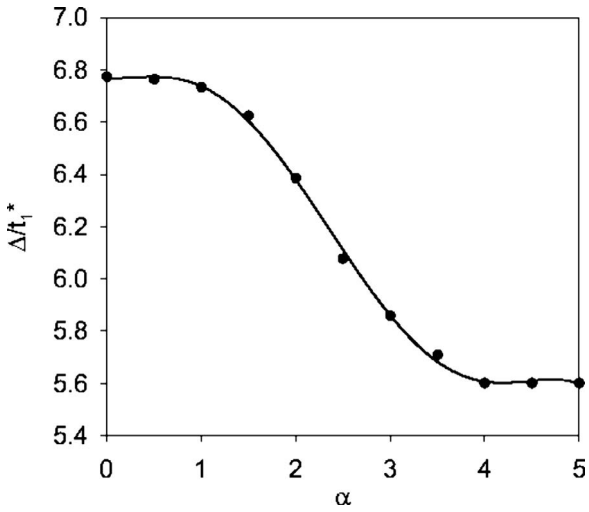

FIG. 9. Ground-state phase diagram for electrons in a half-filled band versus α for $U/t_1^*=0$. The dots are determined from the numerical solution of the DMFT equations. The lines are guide to the eye.

system.[13] On the other hand, we showed that decreasing the correlated disorder reduces the extended phase.[24] An experimental result in weak one-dimensional random potentials has showed that correlations in weakly disordered potentials can enhance localization for a continuum of states, demonstrating that the long-range correlations may either suppress or enhance localization. In a future work we intend to study correlations in the correlated disorder using the direct diagonalization and the calculation of the participation radius.[25] A previous work[14] about phase separation in the particle-hole asymmetric Hubbard model involving NNN hoppings suggests that the inclusion of the temperature in determining the (U,T,μ) phase diagram is crucial for the study of the Anderson localization in a disordered electron system described by the Falicov-Kimball model. We will analyze these effects in future works.

ACKNOWLEDGMENTS

Financial support of Conselho Nacional de Pesquisas Científicas (CNPq) is gratefully acknowledged. H.J.H. acknowledges the Max Planck prize. A.M.C.S. is grateful to the International Centre for Theoretical Physics (Trieste, Italy) for support and hospitality during his visit from January to March 2008.

[1] F. X. Bronold, A. Alvermann, and H. Fehske, Philos. Mag. **84**, 673 (2004).
[2] A. Alvermann and H. Fehske, Eur. Phys. J. B **48**, 295 (2005).
[3] G. Schubert, A. Weisse, and H. Fehske, Phys. Rev. B **71**, 045126 (2005).
[4] N. F. Mott, Proc. Phys. Soc., London, Sect. A **62**, 416 (1949).
[5] V. Dobrosavljevic and G. Kotliar, Phys. Rev. Lett. **78**, 3943 (1997).
[6] R. Abou-Chacra, P. W. Anderson, and D. J. Thouless, J. Phys. C **6**, 1734 (1973).
[7] P. W. Anderson, Phys. Rev. **109**, 1492 (1958).
[8] K. Byczuk, W. Hofstetter, and D. Vollhardt, Phys. Rev. Lett. **94**, 056404 (2005).
[9] K. Byczuk, Phys. Rev. B **71**, 205105 (2005).
[10] E. W. Montroll and M. F. Schlesinger, J. Stat. Phys. **32**, 209 (1983).
[11] M. Romeo, V. Da Costa, and F. Bardou, Eur. Phys. J. B **32**, 513 (2003).
[12] V. Dobrosavljevic, A. A. Pastor, and B. K. Nikolic, Europhys. Lett. **62**, 76 (2003).
[13] A. M. C. Souza, D. O. Maionchi, and H. J. Herrmann, Phys. Rev. B **76**, 035111 (2007).
[14] M. Eckstein, M. Kollar, M. Potthoff, and D. Vollhardt, Phys. Rev. B **75**, 125103 (2007).
[15] J. E. Hirsch, Phys. Rev. B **71**, 104522 (2005).
[16] M. J. Rozenberg, G. Kotliar, H. Kajueter, G. A. Thomas, D. H. Rapkine, J. M. Honig, and P. Metcalf, Phys. Rev. Lett. **75**, 105 (1995).
[17] M. Eckstein, M. Kollar, K. Byczuk, and D. Vollhardt, Phys. Rev. B **71**, 235119 (2005).
[18] M. Paczuski, S. Maslov, and P. Bak, Phys. Rev. E **53**, 414 (1996).
[19] F. A. B. F. de Moura and M. L. Lyra, Phys. Rev. Lett. **81**, 3735 (1998).
[20] C. A. Macedo, L. G. Azevedo, and A. M. C. de Souza, Phys. Rev. B **64**, 184441 (2001).
[21] K. Leung and F. S. Csajkall, J. Chem. Phys. **108**, 9050 (1998).
[22] K. Slevin and T. Ohtsuki, Phys. Rev. Lett. **82**, 382 (1999).
[23] H. Grussbach and M. Schreiber, Phys. Rev. B **51**, 663 (1995).
[24] U. Kuhl, F. M. Izrailev, and A. A. Krokhin, Phys. Rev. Lett. **100**, 126402 (2008).
[25] M. Schreiber, Phys. Rev. B **31**, 6146 (1985).